

Supporting Information

Sanz et al. 10.1073/pnas.0911539107

SI Text

SI Materials and Methods. *Drosophila Stocks and Maintenance.* w^{1118} , standard balancer, and *da-GAL4* driver lines were obtained from stock centers (Table S2). Flies were maintained in standard medium with supplements as previously (1).

Generation of UAS-NDI1 Transgenic *Drosophila* Lines. The yeast (*S. cerevisiae*) *NDI1* coding region (2), was amplified from total yeast genomic DNA as a 1542 bp fragment, using gene-specific primers (shown 5'-3') CTATAATCCTTTAAAAAAGTCTCTTTTG and ATGCTATCGAAGAATTGTATAGTAAC, plus Pfu DNA polymerase (Fermentas), and cloned into pCR@-Blunt II-TOPO (Invitrogen). The 5 × UAS element and minimal (Hsp70) promoter were excised from pUAST (3) as a 381 bp *Bam*HI-*Eco*RI fragment and ligated into the polylinker of the *Drosophila* P-element vector pGREEN-H-Pelican [(4), *Drosophila* Genomics Resource Center], cut with *Bg*III and *Eco*RI. Using sites in the polylinker of pCR@-Blunt II-TOPO, the *NDI1* gene was then excised as a *Kpn*I-*Xho*I fragment and ligated into the pGREEN-H-Pelican polylinker cut with the same enzymes. The complete sequence of the *NDI1* construct was then determined and found to be free of any introduced mutations. All restriction digestions were carried out under manufacturer's recommended conditions (NEB, Fermentas). Following microinjection into w^{1118} recipient embryos (VANEDIS *Drosophila* Injection Service), transgenic progeny were established as independent lines in the w^{1118} background. Insertion sites were determined by inverse PCR (1). Lines *NDI1*^{A46} (intergenic insertion on chromosome 3L, nt 1525573 of NCBI database entry NT_037346.4, between the genes *CrebA* (CG7450) and *obst-H* (CG33983), band 71E3 1) and *NDI1*^{B20} (insertion on chromosome 2L, nt 7576671 of NCBI database entry NT_033779.4, inside the promoter region of the gene *Rapgap1* (CG34374), band 28B1) were retained for further study, maintained as hemizygotes using the eye-color marker and appropriate balancers, and used to generate homozygotes where needed for specific experiments and for long-term maintenance. The homozygotes had no detectable phenotype. For backcrossing to the reference strain used in lifespan experiments (Dahomey w^-) virgin females homozygous for the *NDI1* transgene in the w^{1118} background were crossed over 11 generations with Dahomey w^- males. A similar strategy was used to backcross the *da-GAL4* driver into the Dahomey w^- background.

Testing of Toxin Resistance In Vivo. Resistance to antimycin, rotenone or paraquat was assayed essentially as described by Fridell et al. (5). In brief, flies were starved for two hours in empty vials, following which groups of 20 flies (males and females separately) were placed in vials containing Whatman paper (3 cm × 1 cm) impregnated with 5% (w/v) sucrose and the appropriate drug, at concentrations indicated in figure legends. The proportion of flies surviving was recorded over 2–50 h, depending on the drug. Survival was analyzed using either the Kaplan Meier Log-Rank Test for survival curves, and/or *t* test to compare specific time-points between expressing and nonexpressing flies.

RNA Extraction and Quantitation. RNA was isolated as described in Fernandez-Ayala et al. (1), from 3 biological replicate samples of each genotype tested. Two μg of total RNA was used for cDNA synthesis, which was performed using the High Capacity cDNA Reverse Transcription Kit (Applied Biosystems), according to the manufacturer's recommended conditions. cDNA was synthesized in triplicates, which were subsequently pooled and diluted 1:20

for Q-RT-PCR. Expression of *NDI1* was measured relative to that of housekeeping gene *RpL32* using the StepOnePlus™ Real-time PCR instrument (Applied Biosystems) and the manufacturer's Fast SYBR® Green reagents and recommended conditions, with primers *NDI1* L2: GGTGGTGGGCTACTGGTGT and *NDI1* R2: TTCAAAACGATGGGCAGAGC for *NDI1*, and *RpL32* F short: AGCCCAAGATCGTGAAGAA and *RpL32* A short: TGTGCACCAGGAAGTTCTTGAA for *RpL32* (all 5'-3'). A series of five-fold dilutions of an external standard was used in each run to produce a standard curve. Each analytical and standard reaction was performed in three technical replicates. Fluorescence data were extracted and analyzed using StepOne Software version 2.0 (Applied Biosystems). The levels of *CG3683* and *CG6020* mRNAs were measured similarly, also using *RpL32* as an internal standard, with the following primer pairs: *CG3683*F: ATCTATCGTCGGCGGCCTTA plus *CG3683*R: CTGCCGGCACAGCATAAAC, and *CG6020*F: ATCATCAACGCCGCAAG plus *CG6020*R: GTCGAC-CAGCTCGTCAACT (all 5' to 3').

Protein Analysis by Western Blots. Subcellular fractionation, protein extraction, SDS-PAGE and Western blotting were essentially as described in Fernandez-Ayala et al. (1). Antibodies used in Western blots, together with appropriate secondary antibodies, were as follows: rabbit polyclonal against *Ndi1p* (6), used at 1:15,000 dilution; against bovine heart complex I *NDUFS3* subunit—mouse monoclonal, MitoSciences, catalogue No. MS112, used at 1:20,000; against human recombinant pyruvate dehydrogenase (PDH) E1α subunit—mouse monoclonal, MitoSciences, catalogue No. MSP07, used at 1:10,000; against bovine complex V ATP synthase subunit α (ATPα)—mouse monoclonal, MitoSciences, Catalogue No. MS507, used at 1:75,000; against human GAPDH (C terminus)—goat polyclonal, Everest Biotech, Catalogue No. EB06377, used at 1:30,000. Secondary antibodies used were HRP-conjugated goat antirabbit (BioRad) at 1:10,000 dilution, HRP-conjugated horse antimouse IgG [H + L], Vector Laboratories, Catalogue No. PI-2000, used at 1:10,000; and donkey antigoat IgG-HRP, Santa Cruz Biotechnology, Catalogue No. sc-2020, used at 1:5,000. The antibody against *Ndi1* and its use are described in the main text.

Blue Native-Polyacrylamide Gel Electrophoresis (BNE) and In-Gel Histochemistry. BNE was performed using NativePAGE™ Novex® 3–12% Bis-Tris Gels. Mitochondria were isolated according to Fernandez-Ayala et al. (1). Aliquots of 100 μg of mitochondrial protein were dissolved in a final volume of 40 μl 750 mM aminocaproic acid (in 50 mM Bis-Tris) and 5 μl of 10% dodecylmaltoside were added. Samples were incubated for 10 min on ice, and centrifuged for 15 min at 12,000 g_{max} at 4°C. Supernatants were decanted to a fresh tube and 2.5 μl of cold sample buffer (500 mM aminocaproic acid, 5% Serva Blue G) were added. After an incubation of 5 min on ice, samples of 12 μl (i.e. containing approximately 30 μg of protein) were loaded on each lane. Electrophoresis was performed for 1 h 30 min at 4°C at 75 V, after which blue cathode buffer (cathode buffer +0.02% Serva Blue G) was replaced by cathode buffer (50 mM Tricine, 15 mM Bis-Tris), and the electrophoresis was continued for 5 h at 100 V. For total quantification of respiratory complexes, gels were fixed and stained in stain solution (50% methanol, 10% acetic acid, 0.1% Serva Blue G) for 1 h, then destained for 30 min in destain solution (50% methanol, 10% acetic acid). For in-gel assay of complex I (7), gels were incubated in complex I activity buffer

(2 mM Tris, 0.1 mg/ml NADH, 2.5 mg/ml Nitroblue tetrazolium chloride, pH 7.4) for 20 min, after which they were fixed in destain solution for 20 min. For in-gel assay of complex IV (7), gels were incubated in complex IV activity buffer (5 mg 3,3'-diamidobenzidine tetrahydrochloride (DAB) dissolved in 9 ml phosphate buffer (0.05 M, pH 7.4), 1 nM catalase (20 µg/ml), 10 mg cytochrome *c*, and 750 mg sucrose) for 2 h, after which they were fixed in destain solution for 20 min. All activity staining was carried out at room temperature. The band intensities of both protein content and complex I activity were estimated by optical densitometry.

NADH Dehydrogenase Assay. Mitochondria, isolated by the standard procedure (1) and resuspended in 100 µl, were disrupted by sonication (BioRad Bioruptor™ at high setting, 30 s on, 30 s off for 3 min) to allow the access of NADH to the respiratory complexes. Aliquots of 0.25 mg/ml of mitochondrial protein were used in 1.5 ml of assay buffer containing BSA (120 mM KCl, 5 mM KH₂PO₄, 3 mM Hepes, 1 mM EGTA, 1 mM MgCl₂, 0.2% BSA, pH 7.2) in a cuvette with a magnetic stirrer at a controlled temperature of 25 °C. Ten µl NADH (final concentration 26.66 µM) was added to the cuvette and the NADH oxidation rate was measured. After all the NADH was consumed 3 µl of rotenone (final concentration 5 µM) was added to inhibit complex I, and another 10 µl of NADH were added, with or without the further addition of KCN to 100 µM, to assay rotenone-resistant NADH oxidation.

Polarography and Assay of Mitochondrial H₂O₂ Production. Mitochondria were isolated and used to measure substrate oxidation rates by polarography as previously (1), with substrates and inhibitors as indicated (20 mM sn-glycerol 3-phosphate, 5 mM sodium pyruvate plus 5 mM proline, 10 µM antimycin, 100 µM KCN and rotenone at 5 µM except where indicated). Mitochondrial ROS production was assayed as previously (1) by measuring the generation of hydrogen peroxide in solution in the presence of superoxide dismutase (SOD). For some experiments we adapted our standard mtROS measurement method (1) to a microplate-reader format, (Plate Chameleon V, Hidex) to measure simultaneously all samples in a kinetic assay at 25 °C. Briefly, mitochondrial H₂O₂ production was determined fluorometrically (excitation wavelength = 313 nm, emission wavelength = 420 nm) using a homovanillic acid/peroxidase system in black 96-well plates. Mitochondria (0.15 mg/ml) were incubated in 100 µl of assay buffer (120 mM KCl, 5 mM KH₂PO₄, 3 mM Hepes, 1 mM EGTA, 1 mM MgCl₂, 0.2% bovine serum albumin, pH 7.2 at 25 °C) containing 0.1 mM homovanillic acid, 9 U/ml horseradish peroxidase, and 50 U/ml SOD. Substrates used were pyruvate plus proline (5 mM each) in combination with different inhibitors of the electron transport chain: 5 µM rotenone, 3 µM myxothiazol, 10 µM antimycin, or 100 µM KCN. The reaction was initiated by the addition of the substrate and followed during one hour. The slope of the increase in fluorescence was converted to the rate of H₂O₂ production using a glucose/glucose oxidase calibration system. Three different samples of mitochondria were used from females of each genotype to be analyzed. Samples were analyzed in duplicate and blanks (with exactly the same composition but without substrates) were subtracted. Where indicated in figure legends, we used the ultrasensitive dye Amplex Red (Invitrogen, Carlsbad), according to manufacturer's recommendations (50 mM Amplex Red, 0.1 U/ml peroxidase, excitation: 530 nm, emission: 590 nm) as an alternative method to measure H₂O₂ production.

Assay of Respiration in Crude Homogenates of Adult Flies. Aliquots of 60 flies of each sex and genotype to be tested were placed in a

2 ml tube and minced with scissors for approx 5 min in 2 ml Respiration Buffer A (10 mM Tris-HCl, 300 mM mannitol, 10 mM KCl, 10 mM KH₂PO₄, 5 mM MgCl₂, 1 mg/ml BSA (pH 7.4)). The homogenates were centrifuged at 300 *g*_{max} for 5 min, after which the supernatant was removed and the pellet resuspended in 2 ml Respiration Buffer A. After a second centrifugation, the pellet was resuspended in 1 ml Respiration Buffer A, and 500 µl of the homogenate was transferred to an oxygraph cuvette, followed by the addition of substrates to final concentrations of 5 mM pyruvate, 5 mM proline, and 1 mM ADP. Oxygen consumption was measured, with addition of KCN to a final concentration of 100 µM KCN after approximately 3 min. Rotenone was added to the remaining 500 µl of the homogenate to a final concentration of 1.2 µM, after which samples were incubated at room temperature for 30 min. The oxygen consumption of the rotenone-treated samples was then measured in the same way as untreated samples, before and after the addition of KCN.

NAD⁺/NADH Quantitation. Nicotinamide nucleotide concentrations were determined as described by Balan et al. (8), except that whole flies were used (10 males or 8 females, 2–3 d old).

Lifespan Studies. One hundred flies of each sex were used for each study. Each independent study was repeated twice: Data were pooled and analyzed together. Flies were collected within 24 h of eclosion using CO₂ anesthesia and kept at a density of 20 flies per vial at 25 °C in a controlled 12 h light-dark cycle on standard medium except where stated. Every 2–3 d vials were changed and the number of dead flies was counted, from which median, mean and maximum lifespan (MLS, the last 10% of surviving flies) were calculated. For dietary restriction experiments the same protocol was applied, although the food of the control group (1 yeast: 1 sugar, 1Y:1S) and the group under dietary restriction (0.5 yeast: 0.5 sugar, 0.5Y:0.5S) was prepared according to Mair et al. (9). In our hands, this experimental protocol significantly increases mean, median and maximum lifespan of wild-type flies. Prism GraphPad software was used to construct survival curves that were further analyzed using the Kaplan Meier Log-Rank Test. Mean and maximum life span were further analyzed by ANOVA with Dunnett's Multiple Comparison Test, with *NDI*-expressing flies as test group.

Assay of Sirtuin Activity. Sirtuin activity was assayed in fly homogenates, based on the deacetylation of the substrate Fluor de Lys-SIRT1 (Enzo Life Sciences, Farmingdale, NY, USA), a peptide comprising amino acids 379-382 of human p53 [ArBML-GHis-Lys-Lys(AC)]. The assay's fluorescence signal (excitation 360 nm, emission 460 nm) is generated in proportion to the amount of deacetylation of the lysine corresponding to Lys-382, a known in vivo target of human SIRT1 (homologue of *Drosophila* Sir2). Ten flies per sample were homogenized in extraction buffer (0.1 M Tris-HCl pH 7.4 containing 0.5% Triton X-100, 5 mM β-ME, 0.1 mg/ml PMSF) and placed immediately on ice. Homogenates were centrifuged 15 min, at 2000 *g*_{max} and 4 °C. Supernatants were transferred to a fresh tube where protein concentration was estimated by the Bradford assay, and samples were diluted 1:10 in 40 mM sodium phosphate. Sirtuin activity was assayed using a microplate-reader (Plate Chameleon V, Hidex) containing 0.1 mg/ml of sample in a total volume of 40 µl. Reactions were started by the addition of 10 µl of Fluor de Lys-SIRT1 (10 µM) and followed during one hour. Kinetic rates were calculated using MikroWin 2000 (MikroteK Laborsysteme GMBH) and results expressed as UF per min. To evaluate the specificity of the assay, control samples were incubated in presence of either an activator (10 µl 0.1 µM Resveratrol) or an inhibitor (10 µl 0.1 µM suramin) of Sir2. Fluorescence was increased 47% and inhibited 40% by the

drugs, respectively. No increase in fluorescence was detected in the absence of Fluor de Lys-SIRT1.

Apoptosis Assay in Brain Sections Using TUNEL Staining. Fly heads were fixed with 4% neutral buffered formaldehyde solution, dehydrated and paraffin embedded. Horizontal 4 μ m sections of the brains were stained using the Promega DeadEnd™ fluorometric TUNEL system according to the manufacturer's instructions and mounted in ProLong® GOLD antifade reagent (Invitrogen), containing DAPI as a counterstain for nuclei. Images were taken at 150 \times magnification using an Olympus IX70 confocal microscope with Andor IQ imaging software, and cropped, rotated, and compressed with Adobe Photoshop CS4.

Analysis of Protein Oxidative Damage Markers by Mass Spectrometry. The levels of markers of protein oxidation [the protein carbonyl amino adipic semialdehyde (AASA)], glycooxidation [carboxymethyl-lysine (CML)], and lipoxidation [malondialdehydelysine (MDAL)] were determined by gas chromatography/mass spectrometry (GC/MS). The trifluoroacetic acid methyl ester derivatives of these markers were measured in acid-hydrolyzed, delipidated and reduced protein samples using an isotope dilution method as previously described (10) with an HP6890 Series II gas chromatograph (Agilent), a MSD5973A Series and a 7683 Series automatic injector, an HP-5MS column (30-m \times 0.25-mm \times 0.25- μ m), and the described temperature program (10). Quantification was performed by external standardization using standard curves constructed from mixtures of deuterated and nondeuterated standards. Analyses were carried out by selected ion-monitoring GC/MS (SIM-GC/MS). The ions used were: lysine and [$^2\text{H}_8$]lysine, m/z 180 and 187, respectively; 6-hydroxy-2-aminocaproic acid and [$^2\text{H}_4$]6-hydroxy-2-aminocaproic acid (stable derivatives of AASA), m/z 294 and 298, respectively; CML and [$^2\text{H}_4$]CML, m/z 392 and 396, respectively; and MDAL and [$^2\text{H}_8$]MDAL, m/z 474 and 482, respectively. The amounts of product were expressed as the μ molar ratio per mol of lysine. Between 5–7 samples (100 flies per sample) were analyzed in each group.

Genetic Nomenclature. In text, figures, and legends, *NDI1*^{A46} and *NDI1*^{B20} indicate the two transgenic insertions of *NDI1*, on chromosomes 3 and 2, respectively. *NDI1*^{A46}/3 and *NDI1*^{B20}/2 denote these transgenes in combination with wild-type chromosomes 3 or 2, respectively. 2/2 and 3/3 denote flies homozygous for wild-type chromosomes 2 or 3, respectively. *da-GAL4*/3 similarly denotes flies heterozygous for the *da-GAL4* driver on chromosome 3. Where not stated, *NDI1* “transgene only” flies were of genotype 2/2; *NDI1*^{A46}/3 for transgene *NDI1*^{A46} and of genotype *NDI1*^{B20}/2; 3/3 for transgene *NDI1*^{B20}. In combination with *da-GAL4* to drive ubiquitous expression, the corresponding genotypes were 2/2; *NDI1*^{A46}/*da-GAL4* and *NDI1*^{B20}/2; *da-GAL4*/3, or 2/2; *AOX*^{F6}/*da-GAL4* where *AOX* was expressed instead (e.g., Fig. 1B). *CyO* and *Sb* denote the standard markers present on balancer chromosomes for chromosome 2 and 3, respectively.

Image Processing. Western blot and gel images were cropped to show relevant bands. In some cases brightness and contrast were adjusted to make the images optimally visible, but no gamma correction was performed. Nonadjacent tracks of the same gel, or reprobings with different antisera are shown separately. BNE gels stained for different activities were run in parallel.

Extended Versions of Figure Legends from Main Article Text Fig. 1 Expression of *NDI1* in *Drosophila* is benign. (A) Mean eclosion day \pm SEM (4 replicate experiments) of progeny from a cross between *da-GAL4*/*Sb* females and males hemizygous for the *NDI1*^{A46} transgene, all in the w1118 background. Progeny classes were

distinguished by eye color and bristle morphology (*da-GAL4* and *NDI1* transgenes both confer orange eye color in the w1118 background). $n = 1827$ males, 1978 females. There were no significant differences between classes (ANOVA, $p > 0.05$). For similar experiments using the *NDI1B20* transgenic line see Fig. S1. (B) Q-RT-PCR of *NDI1* RNA from flies of indicated sex and genotype, normalized to that of endogenous *RpL32*. In nontransgenic flies the signal was below the detection limit. (C) Western blots of total (T) mitochondrial (M) and cytosolic (C) protein extracts from *NDI1*-expressing and nonexpressing flies of sex and genotype as shown, probed with antibodies as indicated. The *Ndi1* antibody cross-reacted very weakly with an unidentified polypeptide, in addition to bona fide *Ndi1* which was detected only when transgene expression was driven by *da-GAL4*. Expressed *Ndi1* co-fractionated with the mitochondrial (ATP α), not the cytosolic marker (GAPDH).

Fig. 2 *NDI1* creates rotenone-resistant NADH dehydrogenase activity and decreases ROS production. NADH dehydrogenase activity in mitochondrial extracts from flies of the sex and genotypes indicated, in the absence (A) or presence (B) of 5 μ M rotenone. * indicates significantly different data classes (ANOVA, $p < 0.001$). (C) ROS production (nmol H₂O₂/min mg prot) from suspensions of mitochondria from flies of the sex and genotypes indicated, in the presence of substrates and inhibitors shown. * indicates significantly different data classes (ANOVA, $p < 0.001$). See also Fig. S2. (D) NAD⁺/NADH ratio in homogenates of flies of the sex and genotypes indicated (means \pm SD, t test comparing expressors and nonexpressors of the same sex, $p < 0.001$ indicated by *). *NDI1* only indicates presence of the transgene without driver.

Fig. 3 *NDI1* can compensate for complex I deficiency in *Drosophila* in vivo. (A) Mean proportions of each progeny class (\pm SD, 2 replicate experiments) expressed as percentages of the expected proportion (in each case one quarter of all progeny of the given sex), eclosing from cross between females hemizygous for both the specified RNAi and *NDI1A46* transgenes over the indicated balancers, and males homozygous for *da-GAL4*. The RNAi knockdown targets were CG3683 ($n = 423$ total progeny) and CG6020 ($n = 673$ total progeny) as indicated. No progeny eclosed in either case when knockdown was effected by *da-GAL4* alone (progeny class 3), but substantial numbers of progeny were obtained when the *NDI1* transgene was coexpressed (progeny class 4). See also Fig. S3 D and E. (B) Verification of knockdown at the RNA level by Q-RT-PCR. Data are normalized for each target gene to its expression level in progeny flies from the same cross lacking interfering RNA (for full data see Fig. S3F). (C) Verification of knockdown at the protein level. BNE gels of mitochondrial protein extracts from flies of the sex and genotype as shown, stained as indicated (cI-V—complex I-V, sc—super-complexes). Knockdown of either CG3683 (here) or CG6020 (Fig. S3H) resulted in an almost complete absence of assembled, active complex I.

Fig. 4 *NDI1* expression increases lifespan independently of dietary restriction. (A) Lifespan curves for male flies of the genotypes indicated, in the Dahomey w⁻ background, on different media as shown. Flies indicated as *NDI1* + *da-GAL4* are of genotypes 2/2; *NDI1A46*/*da-GAL4* and *NDI1B20*/2; *da-GAL4*/3, respectively, for the two *NDI1* transgenic lines. Plotted data are from two independent experiments, each with 100 flies per genotype cultured on each medium. All lines were studied in parallel, but for clarity, data for the two transgenic lines are shown independently, together with the controls. Dotted lines indicate extrapolation of median lifespan. Lifespans [median, mean, maximum d] of the different groups were as follows: On rich medium (1Y:1S):

NDIIA46 + da-GAL4 [64, 59, 77], *NDIIA46* only [49, 46, 67], *NDIIB20 + da-GAL4* [60, 57, 70], *NDIIB20* only [43, 43, 67], *da-GAL4* only [52, 50, 71], wild-type [45, 44, 66]. Under dietary restriction (0.5Y:0.5S): *NDIIA46 + da-GAL4* [76, 70, 85], *NDIIA46* only [56, 54, 73], *NDIIB20 + da-GAL4* [73, 67, 81], *NDIIB20* only [57, 53, 72], *da-GAL4* only [60, 57, 76], wild-type [51, 49, 69]. Median, mean, and maximum lifespan of *NDII*-expressing flies was significantly higher (log-rank test $p < 0.01$; ANOVA $p < 0.01$) than the corresponding control groups on both media, with the sole exception of maximum lifespan of transgenic line *NDIIB20* on rich medium, where no significant differences was seen from *da-GAL4* only flies (ANOVA, $p > 0.05$). In all cases, dietary restriction increased median (log-rank test, $p < 0.001$), mean and maximum (ANOVA, $p < 0.01$) lifespan. See also Fig. S4. (B) Sirtuin activity in homogenates of young (1–5 d) and old (30 d males, 50 d females) flies of the sex and genotypes indicated. * indicates significantly different data classes (means \pm SEM, ANOVA, $p < 0.05$). UF—units of fluorescence at 460 nm.

Fig. 5 *NDII* expression mitigates mitochondrial ROS production, oxidative damage and brain apoptosis in aging flies. (A) Substrate oxidation, mitochondrial ROS production, and markers of oxidative damage in aging (30 d male, 50 d female) *NDII*-expressing and nonexpressing flies. State 3 oxygen consumption was measured in isolated mitochondria in the presence of pyruvate+proline+sn-glycerol-3-phosphate substrate mix, ROS production from mitochondrial suspensions in the presence of pyruvate+proline as substrate and detected using Amplex

Red. Markers of oxidative damage to proteins (MDAL—malondialdehyde-lysine, CML—carboxymethyl-lysine). * indicates statistically significant differences between expressing and nonexpressing flies of the same sex (means \pm SEM, t test, $p < 0.05$ for substrate oxidation and oxidative damage, $p < 0.01$ for ROS production). See also Fig. S5. (C). Apoptosis in brain sections from aged females (77 d) of the indicated genotypes. Apoptotic nuclei stained by TUNEL, counterstained by DAPI as indicated. See also Table S1.

Note on Author Contributions A.S. performed behavioral and biochemical analyses and lifespan curves, and cosupervised the project. M.S. constructed transgenic construct, mapped insertion sites, and conducted preliminary phenotypic analyses of transgenic lines. A.W. performed biochemical analyses and lifespan curves. E. Kemppainen co-devised the cloning strategy, and assisted with insertion site analyses and preliminary phenotypic analyses. G.M. and S.E. performed behavioural and biochemical analyses. K.K.K. assisted with Q-RT-PCR analyses. R.S. analyzed coexpression of *NDII* and *AOX*. T.T. and M.L. analyzed the rescue of complex I knockdown. E.D. supervised and assisted with biochemical analyses. B.H. performed TUNEL staining on brain sections. E. Kiviranta, A.Z., and S.V. performed Western blot analyses. A.N. and R.P. analyzed oxidative damage markers. M.J., M.P.O., and R.P. analyzed dicarbonyl compounds. A.M.-Y., T.Y., P.R., and R.P. codesigned the project. H.T.J. codesigned and cosupervised the project, compiled the figures, and drafted the manuscript.

1. Fernandez-Ayala DJM, et al. (2009) Expression of the *Ciona intestinalis* alternative oxidase (AOX) in *Drosophila* complements defects in mitochondrial oxidative phosphorylation. *Cell Metab* 9:449–460.
2. Marres CA, de Vries S, Grivell LA (1991) Isolation and inactivation of the nuclear gene encoding the rotenone-insensitive internal NADH: ubiquinone oxidoreductase of mitochondria from *Saccharomyces cerevisiae*. *Eur J Biochem* 195:857–862.
3. Brand AH, Perrimon N (1993) Targeted gene expression as a means of altering cell fates and generating dominant phenotypes. *Development* 118:401–415.
4. Barolo S, Carver LA, Posakony JW (2000) GFP and beta-galactosidase transformation vectors for promoter/enhancer analysis in *Drosophila*. *BioTechniques* 29:726–732.
5. Fridell YW, Sanchez-Blanco A, Silvia BA, Helfand SL (2005) Targeted expression of the human uncoupling protein 2 (hUCP2) to adult neurons extends lifespan in the fly. *Cell Metab* 1:145–152.
6. Seo BB, Nakamaru-Ogiso E, Flotte TR, Matsuno-Yagi A, Yagi T (2006) In vivo complementation of complex I by the yeast Ndi1 enzyme. Possible application for treatment of Parkinson disease. *J Biol Chem* 281:14250–14255.
7. Nijtmans LG, Henderson NS, Holt IJ (2002) Blue Native electrophoresis to study mitochondrial and other protein complexes. *Methods* 26:327–334
8. Balan V, et al. (2008) Life span extension and neuronal cell protection by *Drosophila* nicotinamidase. *J Biol Chem* 283:27810–27819.
9. Mair W, Piper MD, Partridge L (2005) Calories do not explain extension of life span by dietary restriction in *Drosophila*. *PLoS Biol* 3:e223.
10. Magwere T, et al. (2006). Flight activity, mortality rates, and lipoxidative damage in *Drosophila*. *J Gerontol A-Biol* 61A:136–145.

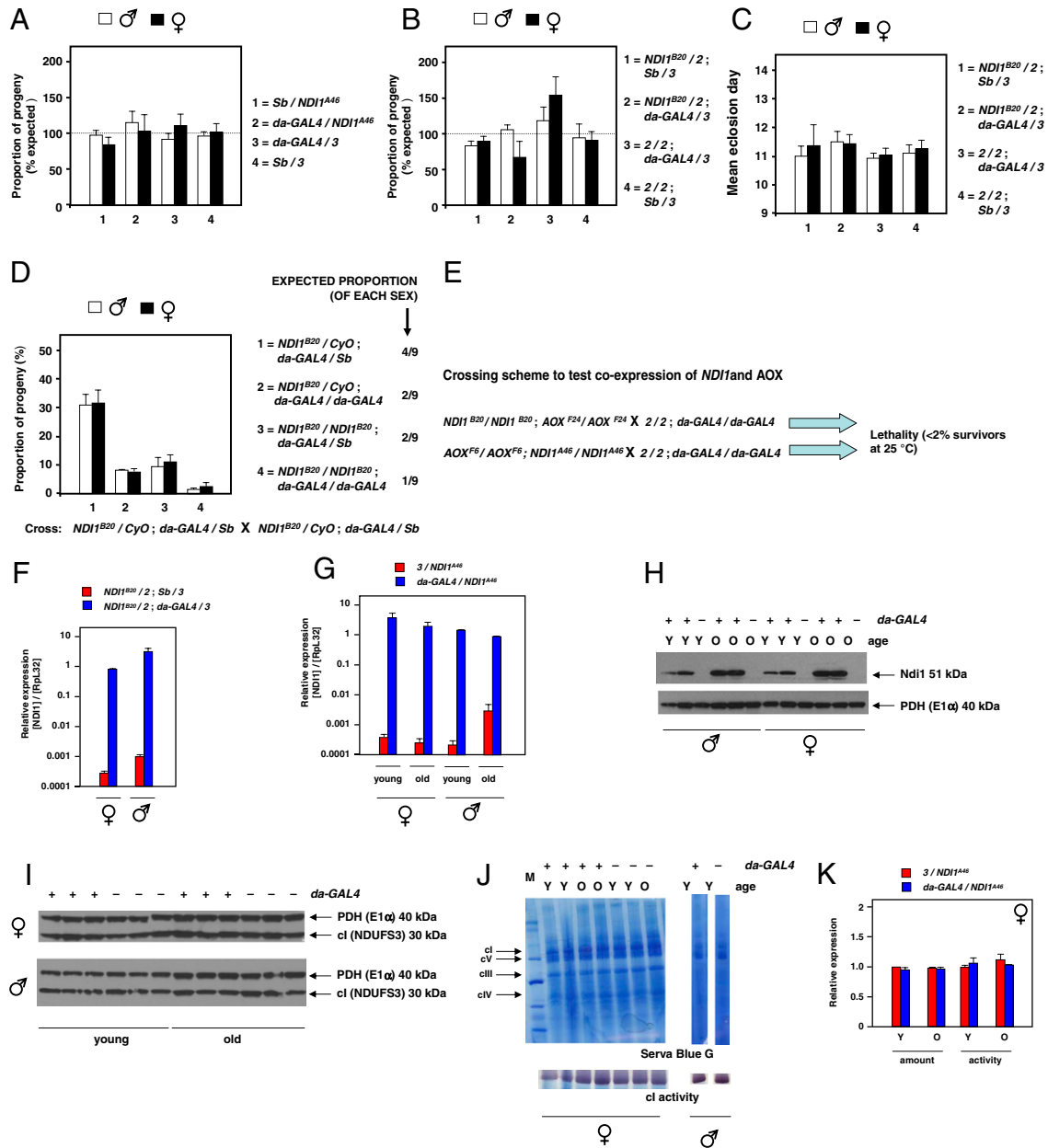


Fig. S1. Expression of *NDI1* in *Drosophila* is benign (A), (B) Mean proportions of each progeny class (\pm SEM, 4 replicate experiments) expressed as percentages of the expected proportion (in each case being one quarter of all progeny of the given sex), eclosing from cross between *da-GAL4/Sb* females and males hemizygous for (A) the *ND1^{A46}* transgene ($n = 1827$ males, 1978 females), and (B) the *ND1^{B20}* transgene ($n = 1848$ males, 1824 females), all in the w^{1118} background. Progeny classes were distinguished by eye color and bristle morphology (*da-GAL4* and *NDI1* transgenes both confer orange eye color in the w^{1118} background). Progeny classes eclosed in the expected 1:1:1:1 ratio in both cases, indicating that *NDI1* expression throughout development is benign. (C) Mean eclosion day \pm SEM (4 replicate experiments) of progeny from the same cross as in (B). There were no significant differences between classes (ANOVA, $p > 0.05$). (D) Proportion (mean percentages \pm SEM, 4 replicate experiments) of progeny of each genotype indicated, eclosing from the cross as shown (transgenic line *ND1^{B20}*). The progeny class carrying two copies of the *NDI1* transgene and one of the *da-GAL4* driver was close to the expected frequency, although the one carrying also two copies of the driver was underrepresented. Note that two copies of either the *CyO* or *Sb* balancer chromosome are lethal, hence 7/16 theoretical progeny classes are missing. (E) Crossing schemes to test for effects of coexpression of *UAS-NDI1* and *UAS-AOX*. Only a tiny number (<2% of the expected number) of flies eclosed under standard growth conditions at 25 °C, with a long developmental delay, and were small. In effect, the two transgenes can be considered synthetically lethal under these conditions. (F), (G) Q-RT-PCR of *NDI1* RNA from flies of indicated sex and genotype, normalized to that of endogenous *RpL32*. The *NDI1* transgene was expressed in both transgenic lines, and expression at the RNA level was seen in both young (1–5 d) and old (30 d old males, 50 d old females) flies. (H) Western blot of mitochondrial protein extracts from *NDI1*-expressing and nonexpressing flies (sex and genotypes as shown), probed with antibodies as indicated. The Ndi1 protein was expressed in both young (Y, 1–5 d) and old (O, 30 d old males, 50 d old females) flies, though was present at a higher level in old flies compared with the PDH E1 α subunit loading control. (I) Western blot of mitochondrial protein extracts from *NDI1*-expressing and nonexpressing flies (sex and genotypes as shown), probed with antibodies as indicated. The steady-state level of the complex I protein NDUFS3, detected with the heterologous antibody against the bovine protein, was unaffected by expression of *NDI1* in both young (Y, 1–5 d) and old (O, 30 d old males, 50 d old females) flies compared with the PDH E1 α subunit loading control. (J) BNE gels of mitochondrial protein extracts from *NDI1*-expressing and nonexpressing young (Y, 1–5 d) and old (O, 50 d old female) flies, stained as indicated (cI–V—complex I–V). (K) Quantification (means \pm SEM) of complex I amount and activity, by densitometry of replicate BNE gels of mitochondrial protein extracts from flies of the genotypes and ages shown (Y, 1–5 d, O, 50 d). There were no significant differences (ANOVA, $p > 0.05$, at least 4 replicates of each group).

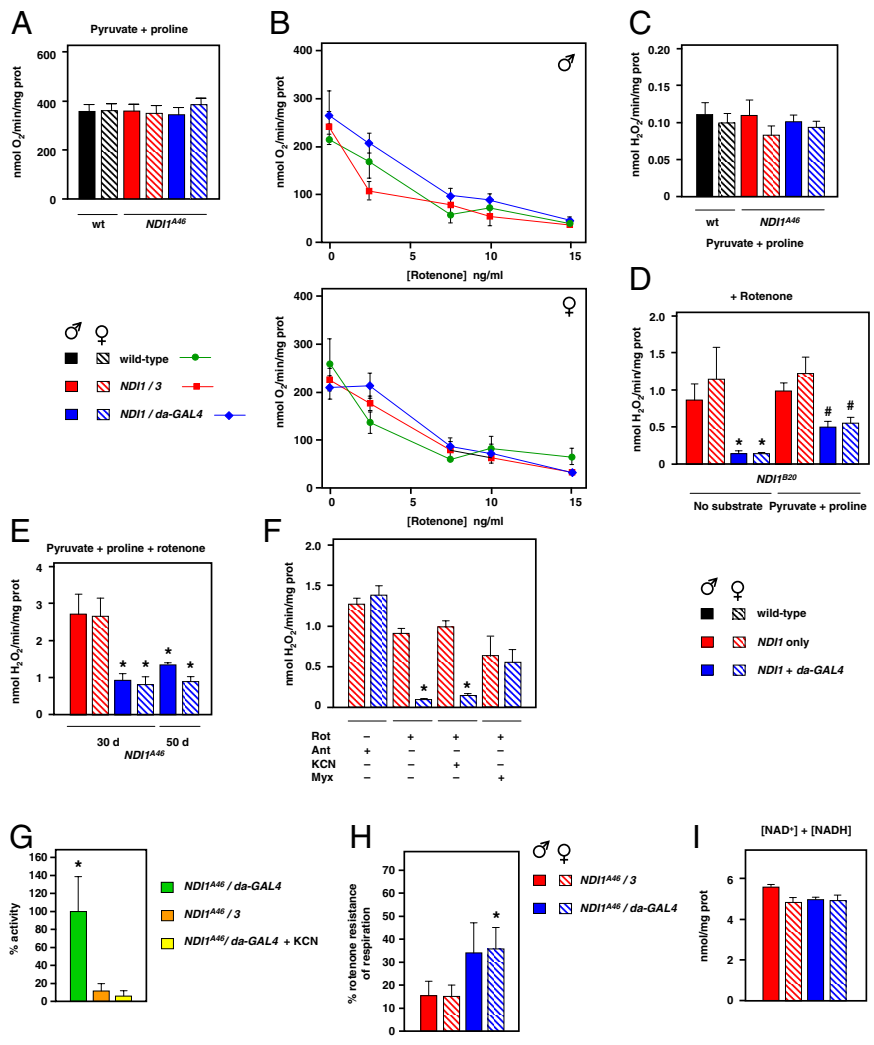


Fig. S2. *NDI1* creates rotenone-resistant NADH dehydrogenase activity and decreases mtROS production. Despite supporting rotenone-resistant NADH dehydrogenase activity (Fig. 2), *NDI1* expression had no significant effect on state 3 oxygen consumption of mitochondrial suspensions from young flies (2–3 d old flies of sex and genotypes indicated, ANOVA, $p > 0.05$), in absence of rotenone (A), or at different concentrations of rotenone (B), using a complex I-linked substrate mix. (C), (D) and (E), ROS production (nmol H₂O₂/min · mg prot) from suspensions of mitochondria from young flies (2–3 d) of the sex and genotypes indicated, in the presence of substrates and inhibitors shown. * and # indicate significantly different data classes (ANOVA, $p < 0.05$). In the absence of rotenone (C), *NDI1* expression had no significant effect on mtROS production in the young flies. (D) Effects on mtROS production using transgenic line *NDI1^{B20}* were as seen for line *NDI1^{A46}* (Fig. 2C). (E) The effect of *NDI1* expression on mtROS production in the presence of rotenone and substrate was maintained in aged flies (30 d or even 50 d). * indicates significantly different data classes (ANOVA, $p < 0.05$). (F) mtROS (H₂O₂) production in females, measured as described in *SI Materials and Methods*, in the presence of various inhibitors as shown. Means ± SEM of 3 biological replicates. * and # indicate significantly different data classes (ANOVA, $p < 0.05$). For noninhibited controls see Fig. S5. (G) NADH dehydrogenase activity in presence of rotenone, in mitochondrial extracts of flies of genotypes as indicated, with or without the additional presence of KCN. Flies of both sexes combined, means ± SD of at least 3 replicates, expressed as a % of the rotenone-resistant activity in extracts of ubiquitously expressing (*NDI1/da-GAL4*) flies. * denotes significantly different data classes (ANOVA, $p < 0.02$). The rotenone-resistant activity was inhibited by cyanide, indicating that in the homogenates used, the activity is dependent upon electron flow into the respiratory chain, mediated presumably via ubiquinone. (H) Respiration in crude homogenates from *NDI1*-expressing and nonexpressing flies of each sex, in the presence of rotenone (1.2 μM), shown as % of the uninhibited respiration rate (means ± SD). The background level of KCN-resistant oxygen consumption, which is assumed to represent nonmitochondrial oxygen usage, is subtracted from the total respiration in each case. Respiration in crude homogenates from *NDI1*-expressing females was significantly different (*) from that in nonexpressing females (*t* test, $p < 0.05$). The corresponding values for males were just outside the borders of significance, but pooled data from both sexes were highly significant ($p < 0.02$). (I) Total amounts (means ± SD) of nicotinamide adenine dinucleotides (NAD⁺ + NADH) in homogenates of whole flies. NADH/NAD⁺ ratios, measured in the same experiment, are shown in Fig. 2D. “*NDI1* only” indicates presence of the transgene without driver. Note that the altered NAD⁺/NADH ratio in homogenates is only an indication, and not a proof, of high NADH dehydrogenase activity inside mitochondria.

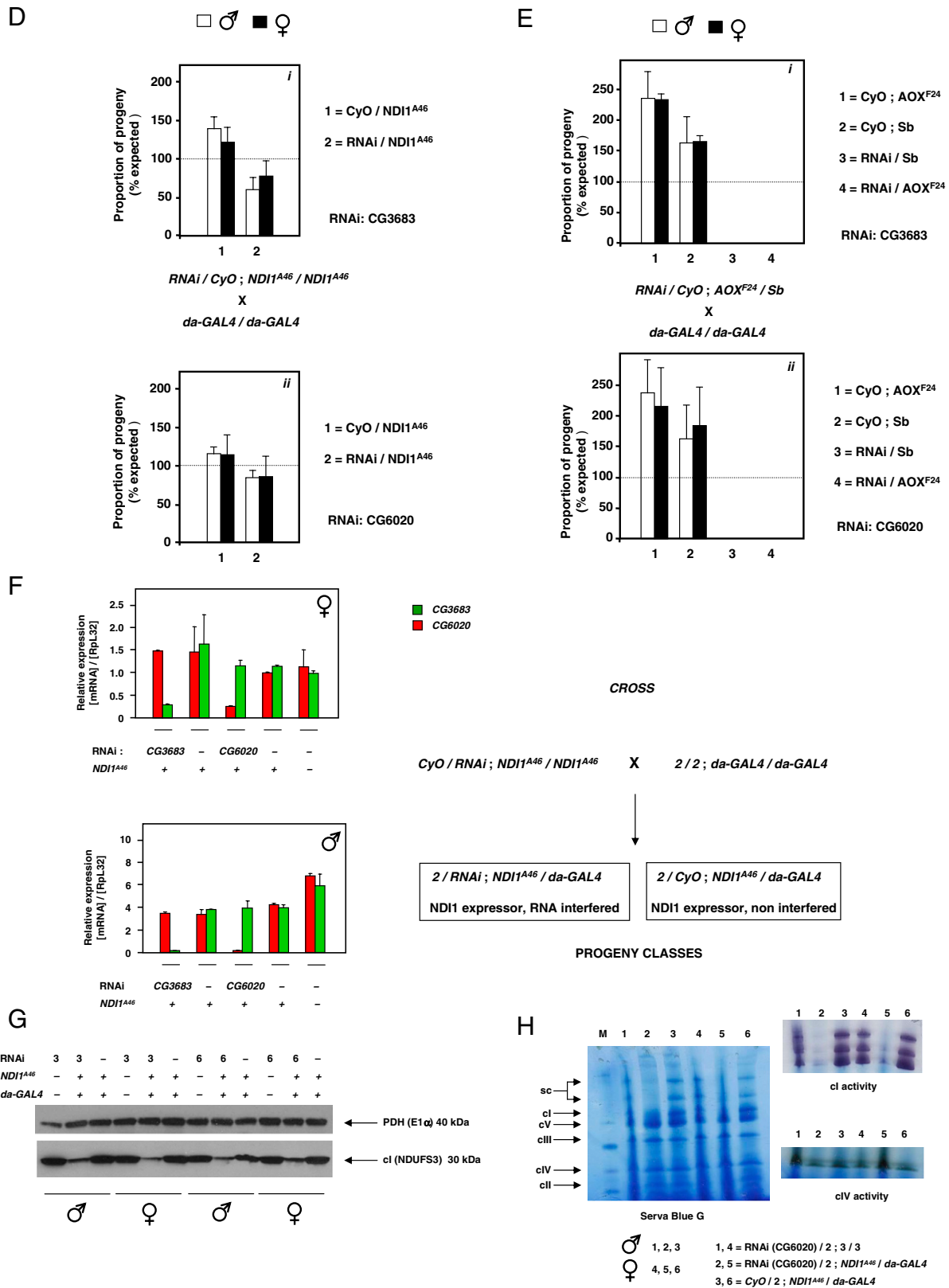


Fig. S3. NDI1 can compensate for complex I deficiency in *Drosophila* in vivo. (A), (B) NDI1 confers partial resistance to rotenone in vivo. Survival curves of (A) male and (B) female flies (2–3 d old) of different genotypes, as indicated, treated with 4 mM (males) or 3 mM (females) rotenone or 3 mM antimycin, all in the same genetic background (Dahomey *w*⁻). Plotted data are means \pm SEM of 5 replicate experiments (20 flies/vial). *NDI1*-expressing flies (open/colored squares) were significantly more resistant to rotenone than nonexpressing controls (black triangles; log-rank test, $p < 0.001$), but not against antimycin (log-rank test, $p > 0.05$). Dotted lines and red arrows indicate extrapolation of LT₅₀ (the time taken for 50% of the flies to die). Yellow ($p < 0.05$) and green ($p < 0.01$) symbols indicate significant differences (*t* test) from corresponding nonexpressing controls. LT₅₀ was 51 min and 55 min for the two lines of *NDI1*-expressing males, but

only 28–29 min for the corresponding nonexpressing control males. Female expressors showed a more modest increase in LT_{50} . LT_{50} in 3 mM antimycin was not increased by *NDI1* expression in either sex. Note that, although the concentrations of rotenone used in this experiment are high compared with those required to inhibit complex I in vitro, when we used lower concentrations (≤ 1 mM) in this procedure, no significant lethality was produced, even after 50 h. Our interpretation is that the toxin “tastes” bad at any concentration, such that the flies only ever ingest a tiny amount of it, resulting in lethality only when highly concentrated solutions are used. (C) *NDI1* confers partial resistance to paraquat in vivo. Survival curves for 10 d old flies of different genotypes, as indicated, treated with 20 mM paraquat. Plotted data are means \pm SEM of 5 replicate experiments (20 flies/vial). Dotted lines and red arrows indicate extrapolation of LT_{50} (the time taken for 50% of the flies to die). Green ($p < 0.01$) and orange ($p < 0.001$) symbols indicate significant differences (t test) from corresponding nonexpressing controls. Flies of all genotypes survived >50 h when supplied with 5% sucrose containing no drug. (D)–(G) *NDI1* rescues lethality due to knockdown of complex I subunits. (D) Mean proportions of each progeny class (\pm SD, 2 replicate experiments) expressed as percentages of the expected proportion (in each case being half of all progeny of the given sex), eclosing from cross between females homozygous for the *NDI^{A46}* transgene and hemizygous for the specified RNAi over the *CyO* balancer, and males homozygous for *da-GAL4*. RNAi knockdown targets were *CG3683* ($n = 711$ total progeny) and *CG6020* ($n = 724$ total progeny) as indicated (see Table S2 for details of the RNAi lines). In both cases substantial numbers of progeny class 2 (with complex I knockdown) eclosed, whereas in repeated control experiments using the original RNAi lines without the presence of *NDI1*, no such progeny eclosed. The result is an additional verification of the conclusions from the more complex experiment shown in Fig. 3A, i.e. that coexpression of *NDI1* rescues the lethality caused by knockdown of essential subunits of complex I. (E) Mean proportions of each progeny class (\pm SD, 2 replicate experiments) expressed as percentages of the expected proportion (in each case being one quarter of all progeny of the given sex), eclosing from cross between females hemizygous for the specified RNAi and *AOX^{F24}* transgenes over the indicated balancers, and males homozygous for *da-GAL4*. RNAi knockdown targets were *CG3683* ($n = 667$ total progeny) and *CG6020* ($n = 550$ total progeny) as indicated. Note that, in contrast to the case with *NDI1*, which rescued the lethality (Fig. 3A), no progeny eclosed when knockdown was effected either by *da-GAL4* alone (progeny class 3), or when the *AOX* transgene was coexpressed (progeny class 4). (F) Details of verification of specific knockdown at the RNA level by Q-RT-PCR. Full data (expression levels normalized to that of the control RNA, Rpl32) for expression of *CG3683* and *CG6020*, in progeny classes as indicated, used to compile the summary data shown in Fig. 3B. (G) Verification of knockdown at the protein level. Western blot of mitochondrial protein extracts from flies of the indicated sex and genotypes (RNAi 3—RNAi against *CG3683*, RNAi 6—RNAi against *CG6020*), probed successively with antibodies against NDUFS3 and the PDH E1 α subunit. (H) Verification of knockdown at the assembly/enzymatic level. BNE gels of mitochondrial protein extracts from flies of the sex and genotypes as shown, stained as indicated (cl-V—complex I-V, sc—supercomplexes). Knockdown of either *CG3683* (Fig. 3C) or *CG6020* (this figure) resulted in an almost complete absence of assembled, active complex I.

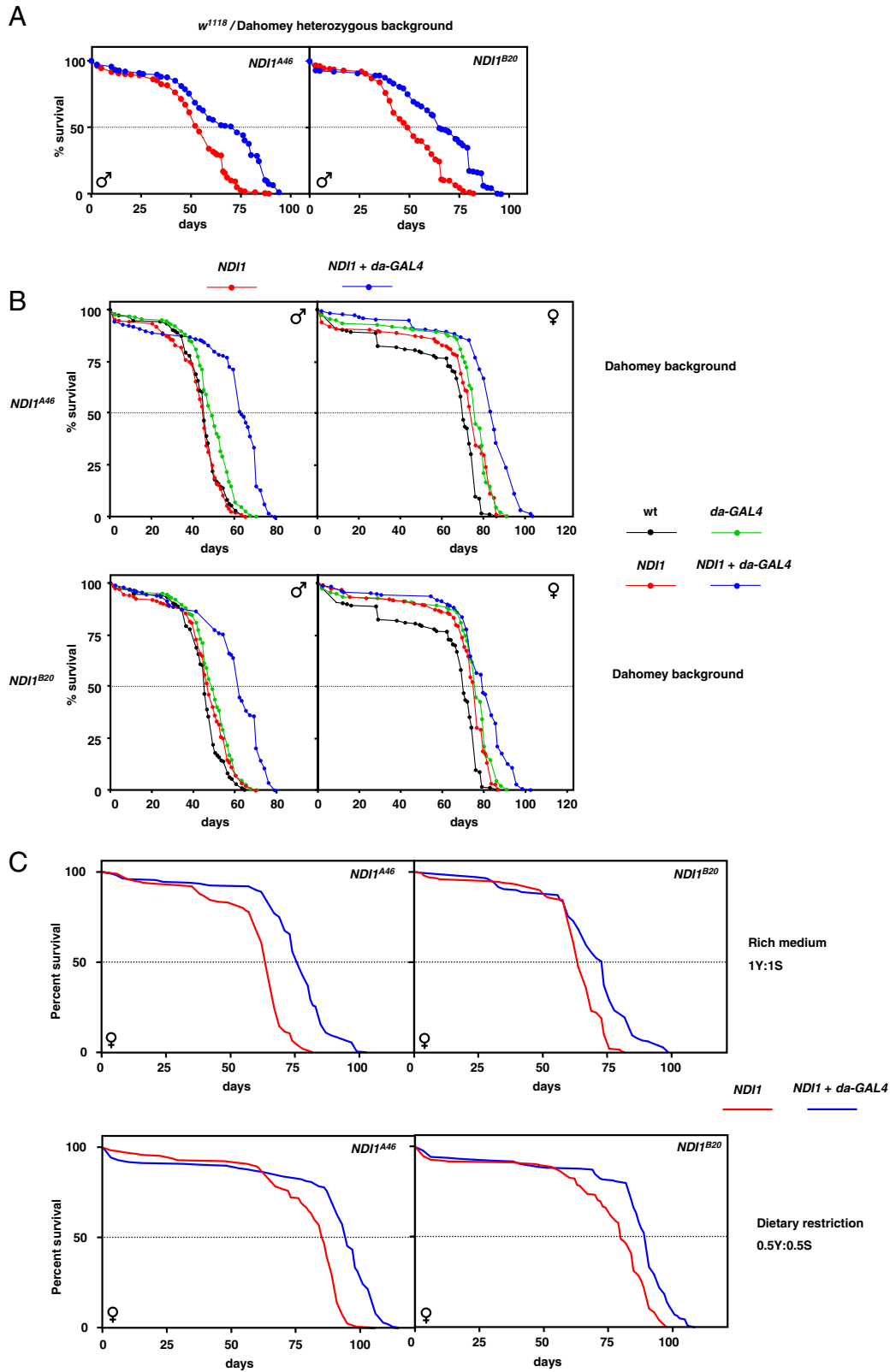


Fig. 54. *NDI1* expression increases *Drosophila* lifespan. (A) Lifespan curves for male flies of the genotypes indicated, in the w^{1118} /Dahomey w^- heterozygous background: *da-GAL4* is carried on chromosome 3, *NDI1^{A46}* is on chromosome 3 and *NDI1^{B20}* on chromosome 2. Flies indicated as *NDI1 + da-GAL4* are thus of genotypes 2/2; *NDI1^{A46}/da-GAL4* and *NDI1^{B20}/2; da-GAL4/3*, respectively for the two strains. Plotted data are from two independent experiments giving similar results, each with 100 flies of each sex per genotype. Lifespans [median, mean, maximum, days] of different groups were as follows *NDI1^{A46} + da-GAL4* [72, 65, 87], *NDI1^{A46} only* [54, 52, 71], *NDI1^{B20} + da-GAL4* [65, 64, 84], *NDI1^{B20} only* [51, 50, 69]. Median, mean and maximum lifespans

of *NDI1* + *da-GAL4* flies were significantly higher (log-rank test $p < 0.001$; t test $p < 0.001$) than nonexpressing controls. Females (not shown) gave qualitatively similar findings: *NDI1^{A46}* + *da-GAL4* [93, 84, 103], *NDI1^{A46}* only [81, 75, 97], *NDI1^{B20}* + *da-GAL4* [93, 79, 106], *NDI1^{B20}* only [89, 78, 100]. Median, mean and maximum lifespans of *NDI1^{A46}* + *da-GAL4* females were significantly higher (log-rank test $p < 0.001$; t test $p < 0.001$) than controls, as were median and maximum lifespans of *NDI1^{B20}* + *da-GAL4* females (log-rank test $p < 0.001$; t test $p < 0.001$). (B) Lifespan curves for flies of the sex and genotypes indicated, in the Dahomey w^- genetic background. Flies indicated as *NDI1* + *da-GAL4* are of genotypes 2/2; *NDI1^{A46}*/*da-GAL4* and *NDI1^{B20}*/2; *da-GAL4*/3, respectively, for the two *NDI1* transgenic lines. Plotted data are from two independent experiments giving similar results, each with 100 flies of each sex per genotype. All lines were studied in parallel, but for clarity, data for the two transgenic lines are shown independently, together with the controls. Dotted lines indicate extrapolation of median lifespan. Lifespans [median, mean, maximum, days] of the different groups were as follows. Males: *NDI1^{A46}* + *da-GAL4* [63, 58, 73], *NDI1^{A46}* only [45, 42, 57], *NDI1^{B20}* + *da-GAL4* [62, 59, 70], *NDI1^{B20}* only [47, 45, 59], *da-GAL4* only [49, 48, 58], wild-type [45, 44, 61]. Females: *NDI1^{A46}* + *da-GAL4* [85, 81, 93], *NDI1^{A46}* only [73, 65, 82], *NDI1^{B20}* + *da-GAL4* [79, 76, 91], *NDI1^{B20}* only [76, 69, 83], *da-GAL4* only [76, 71, 87], wild-type [72, 65, 82]. Median lifespans of *NDI1*-expressing flies of both strains and sexes were significantly different from corresponding control groups (long-rank test, $p < 0.001$). Mean and maximum lifespans of *NDI1*-expressing flies of both strains and sexes were also significantly different from corresponding control groups (ANOVA, $p < 0.01$, except for *NDI1^{B20}* females, $p < 0.05$). (C) Lifespan curves for female *NDI1*-expressor and nonexpressor flies in the Dahomey w^- background, on the indicated media. Plotted data are from two independent experiments, each with 100 flies per genotype cultured on each medium. Lifespans [median, mean, maximum, days] of the different groups were as follows. On rich medium (1Y:1S)—*NDI1^{A46}* + *da-GAL4* [76, 74, 96], *NDI1^{A46}* only [64, 60, 73], *NDI1^{B20}* + *da-GAL4* [69, 69, 87], *NDI1^{B20}* only [64, 62, 69]. Under dietary restriction (0.5Y:0.5S)—*NDI1^{A46}* + *da-GAL4* [95, 87, 105], *NDI1^{A46}* only [86, 79, 95], *NDI1^{B20}* + *da-GAL4* [83, 83, 103], *NDI1^{B20}* only [80, 74, 89]. Median, mean and maximum lifespan of *NDI1*-expressing flies was significantly higher ($p < 0.001$) than the corresponding control groups on both media, and dietary restriction significantly increased median, mean and maximum lifespan of all genotypes tested (log-rank test $p < 0.001$, t test $p < 0.001$).

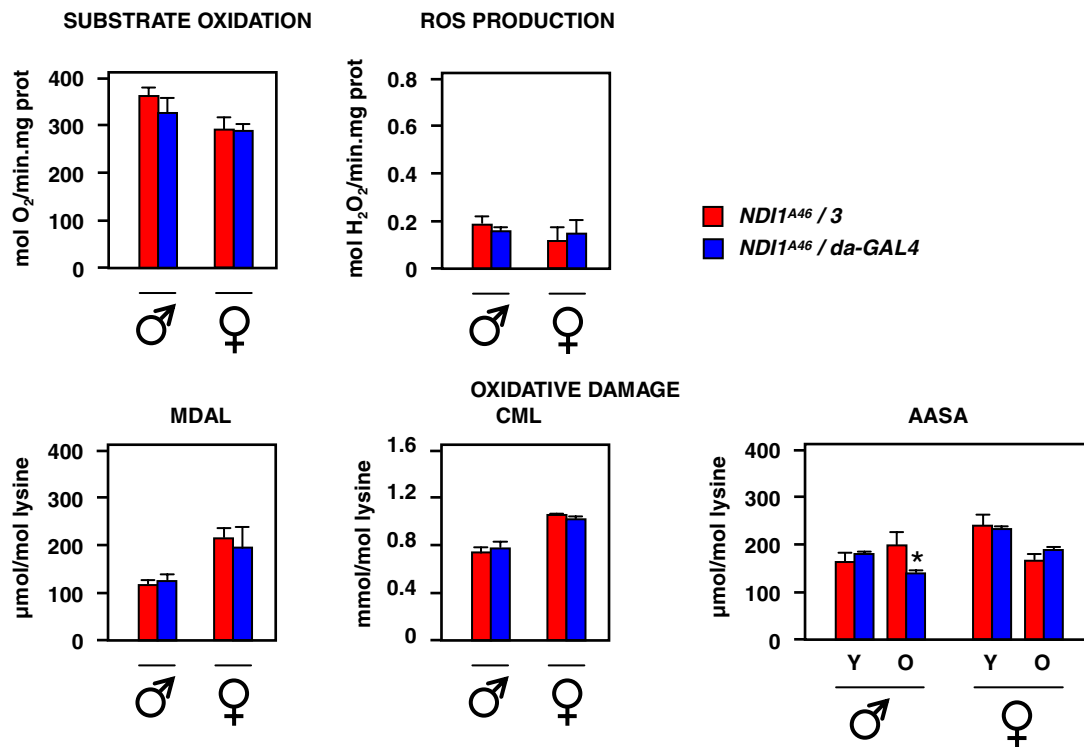


Fig. 55. *NDI1* expression has minimal effects on mitochondrial ROS production and oxidative damage in young flies. Substrate oxidation, mitochondrial ROS production and markers of oxidative damage in young (1–5 d) *NDI1*-expressing and nonexpressing flies of the sex and genotype indicated. State 3 oxygen consumption was measured in isolated mitochondria in the presence of pyruvate + proline + sn-glycerol-3-phosphate substrate mix, ROS production from mitochondrial suspensions in the presence of pyruvate + proline as substrate, and detected using Amplex Red. Markers of oxidative damage (MDAL-malondialdehyde-lysine, CML-carboxymethyl-lysine, AASA-aminoadipic semialdehyde, also shown for aging flies, i.e. 30 d old males and 50 d old females). * indicates statistically significant differences between expressing and nonexpressing flies of the same sex and biological age (means \pm SEM, t test, $p < 0.05$). See also Fig. 5.

Table S1. TUNEL-positive cells in brain sections*

Genotype	Sex	Age (days)	Mean ($n = 3$)	SEM
<i>NDI1^{A46}</i> /3	F	61	0.7	0.67
<i>NDI1^{A46}</i> / <i>da-GAL4</i>	F	61	0	0
<i>NDI1^{A46}</i> /3	F	77	33.0	9.50
<i>NDI1^{A46}</i> / <i>da-GAL4</i>	F	77	4.3	1.67
<i>NDI1^{A46}</i> /3	M	48	0	0
<i>NDI1^{A46}</i> / <i>da-GAL4</i>	M	48	0	0

*Serial slides were produced, but TUNEL staining was performed only on the slides giving the greatest overview of the brain in each case

Table S2. *Drosophila* genomic resources used in the study, together with official database symbol designations and original references

Type of resource	Name used in main text	Official or proposed symbol/genotype in Flybase* or VDRC Transformant ID	Original reference
Transgenic construct	pGREEN-H-Pelican	P{GreenH-Pelican}	1
Transgenic construct	pUAST	P{UAST}	2
GAL4 driver line	<i>da-GAL4</i>	<i>w</i> ⁺ ; P{GAL4- <i>da</i> .G32}UH1	3
AOX transgenic line, insertion on chromosome 3	UAS-AOX (AOX ^{F6} as genotype)	<i>w</i> ¹¹¹⁸ ; P{UAS-AOX; <i>w</i> ⁺ }F6	4
AOX transgenic line, insertion on chromosome 2	UAS-AOX (AOX ^{F24} as genotype)	<i>w</i> ¹¹¹⁸ ; P{UAS-AOX; <i>w</i> ⁺ }F24	4
NDI1 transgenic line, insertion on chromosome 2L, nt 7576671 of NCBI database entry NT_033779.4, inside the promoter region of the gene <i>Rapgap1</i> (CG34374), band 28B1	UAS-NDI1 (NDI1 ^{B20} as genotype)	<i>w</i> ¹¹¹⁸ ; P{UAS-NDI1; <i>w</i> ⁺ }B20	this paper
NDI1 transgenic line, insertion on chromosome 3L at nt 15525573 of NCBI database entry NT_037436, band 71E31, between CG7450 and CG33983	UAS-NDI1 (NDI1 ^{A46} as genotype)	<i>w</i> ¹¹¹⁸ ; P{UAS-NDI1; <i>w</i> ⁺ }A46	this paper
RNAi line targeted against complex I subunit	RNAi: CG3683	VDRC 46797	5
RNAi line targeted against complex I subunit	RNAi: CG6020	VDRC 13131	5

*www.flybase.org

- 1 Barolo S, Carver LA, Posakony JW (2000) GFP and beta-galactosidase transformation vectors for promoter/enhancer analysis in *Drosophila*. *BioTechniques* 29:726–732.
- 2 Brand AH, Perrimon N (1993) Targeted gene expression as a means of altering cell fates and generating dominant phenotypes. *Development* 118:401–415.
- 3 Wodarz A., Hinz U, Engelbert M, Knust E (1995). Expression of *crumbs* confers apical character on plasma membrane domains of ectodermal epithelia of *Drosophila*. *Cell* 82:67–76.
- 4 Fernandez-Ayala DJM, et al. (2009) Expression of the *Ciona intestinalis* alternative oxidase (AOX) in *Drosophila* complements defects in mitochondrial oxidative phosphorylation. *Cell Metab* 9:449–460.
- 5 Dietzl G, et al. (2007). A genome-wide transgenic RNAi library for conditional gene inactivation in *Drosophila*. *Nature* 448:151–156.